FACTA UNIVERSITATIS
Series: **Architecture and Civil Engineering** Vol. 20, Nº 3, 2022, pp. 213-230
https://doi.org/10.2298/FUACE220223017P

Original Scientific Paper

AN ALTERNATIVE NUMERICAL MODEL FOR FIBER REINFORCED CONCRETE STRENGTH EVALUATION

UDC 666.972+677.53
620.173:691.32

Stepa Paunović[1], Aleksandar Šutanovac[2], Predrag Blagojević[2]

[1]Mathematical Institute of the Serbian Academy of Sciences and Arts, Belgrade, Serbia
[2]Faculty of Civil Engineering and Architecture, University of Niš, Serbia

Abstract. *An alternative numerical model for fiber reinforced concrete (FRC) compressive and bending tensile strength determination is presented in this paper. Fibers are modeled explicitly by using the Extended Finite Element Method (XFEM). An alternative method for modeling the fiber-matrix interaction, without the need for additional subroutine definition, is proposed. The presented numerical model was evaluated by experimental tests and results are in good agreement. The model was developed for Simulia ABAQUS software, but the proposed modeling procedure is generally applicable. In the end, some possible model improvements and suggested applications are included.*

Key words: *fiber reinforced concrete, FRC, XFEM, discrete fiber model, fiber-matrix interaction, strength evaluation*

1. INTRODUCTION

1.1. Fiber reinforced concrete and its characteristics

Over the last several decades concrete has become the most widely used construction material in the world and it has been thoroughly studied thus far. One of the main shortcomings of concrete is its low strength when subjected to tension, and the most commonly used way for overcoming this shortcoming is reinforcing the concrete. This can be done in many ways, and the most commonly used one is through the application of steel rebar. However, numerous attempts have been made to find an alternative solution to this problem. One of these solutions is the microreinforced concrete (MRC),

Received February 23, 2022 / Revised December 14, 2022 / Accepted December 15, 2022
Corresponding author: Stepa Paunović, Mathematical Institute of the Serbian Academy of Sciences and Arts, Kneza Mihaila 36, Belgrade 11001, Serbia
e-mail: stepa.paunovic@mi.sanu.ac.rs

which can be MRC in a specific sense, or the fiber reinforced concrete. MRC in a specific sense is obtained when a concrete element is reinforced by some ductile and resilient strips near or on the surface of the element, e.g. [1,2].

Fiber reinforced concrete (FRC) is comprised of concrete matrix and some fibers that are more or less evenly, though randomly dispersed throughout the concrete matrix. One typical cross-section of a FRC element is shown in Figure 1a. These fibers can be of various shapes, sizes and made of various materials. For example, fibers can be couple of millimeters to a couple of centimeters long, straight, spiral or with different types of hooks at the ends, they can be made of steel, polymer, organic fibers, even glass [3]. In fact, one of the most commonly used types are hooked steel or glass fibers [4-7].

Adding fibers to concrete can greatly improve its mechanical characteristics in hardened state. For instance, if fibers are evenly enough distributed in the concrete matrix, the concrete compression strength, tension strength, toughness and ductility will be higher compared to the ordinary, conventional concrete, which has been reported in many researches, e.g. [8-10]. While the increase in concrete strengths can be as high as 80% [8], these fiber reinforced concretes are expansive and they are made only for special uses. For concretes used in practice the increase in strengths varies between 10-20%. However, the main contribution of the added fibers reflects in the dramatic increase of concrete's ductility. In the presence of fibers, depending on their quantity, concrete can be transformed from a very brittle material, to a distinctively ductile material. The described effect becomes most apparent when analyzing a force-displacement diagram or a stress-strain diagram of a structure or element, an example of which is presented in Figure 1b [11]. It can be seen that the post-peak behavior of the plain concrete and the fiber reinforced concrete is quite different – the plain concrete curve is much steeper, implying a more rapid material degradation, while the FRC expresses a very ductile behavior.

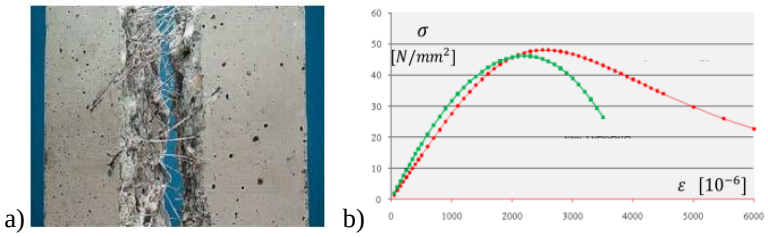

Fig. 1 a) A typical cross section of a fiber reinforced concrete element, b) A stress-strain diagram of a fiber reinforced element [11]

However, mathematical modelling of SFRC is a formidable task. While this challenge can be tackled analytically [12-14], this is applicable only to some simpler problems, while for more detailed solutions and results a numerical model is needed. Nevertheless, although there are several well-developed numerical models for the plain concrete, it is very hard to produce a numerical model that would describe the *fiber reinforced concrete* adequately, due to its highly complex behavior. To this date there is no one generally accepted way for the numerical modeling of fiber reinforced concrete, but there are rather several distinct modeling approaches.

1.2. Numerical modeling of fiber reinforced concrete

The oldest and the most commonly used approach for the numerical modeling of FRC is the modeling of FRC as a homogeneous material [15-21], very similar to conventional concrete modeling, with the appropriate values chosen for influential parameters so that results of numerical analysis would correspond to the results obtained by experimental testing of specimens. Parameters that differ from a conventional concrete model and that have the greatest influence on the behavior of FRC are the parameters related to the adopted concrete stress-strain diagram. The most important of these parameters are the compressive and tensile strength and the elastic modulus of concrete. A more detailed description of influential parameters and their values chosen for modeling FRC in this paper will be given later, while here only the main ideas and key features of different modeling approaches are presented. The mentioned type of modeling FRC is the simplest and also the most numerically effective one (it requires relatively modest computational resources), but on the other hand, it represents a much simplified model of the real material, which is distinctively inhomogeneous. While this model gives satisfactory results when modeling conventional concrete (e.g. [22,23]), for FRC it is much more sensitive to parameter variation and the obtained results depend largely on the right choice of the input parameter values, making it hard to use this model for predicting the FRC behavior without prior experimental tests, thus limiting its application in everyday practice.The next evolution step of numerical FRC modeling is an attempt to combine the advantages of a homogeneous concrete model with high computational power and modern numerical methods available nowadays. Namely, the idea is to model only the concrete matrix as a homogeneous material of appropriate mechanical characteristics, much like in a conventional concrete model, and to model the added fibers discretely, as a system of 1D finite elements (FE) randomly dispersed throughout the concrete matrix, as has been done in [24-27] for instance. An example of this type of modeling is presented in Figure 2 [26]. In this way the use of already well established parameters for concrete is ensured, while avoiding the need for experimental testing required to determine some parameters necessary for formulation of the fully homogeneous FRC model. For this modeling approach, the use of the Extended Finite Element Method (XFEM) is required in order to model the randomly dispersed fibers as *strong discontinuities* in the concrete matrix, while keeping the concrete and fiber FE meshes independent. Although this solution is more precise than the previously described one, it is far more numerically expensive, which again limits its application in everyday engineering practice. Beside this, it is important to define the appropriate fiber-matrix interaction in order to obtain reliable results, and the required data about the fiber-cement interface and interaction are not always available and they should be determined experimentally.

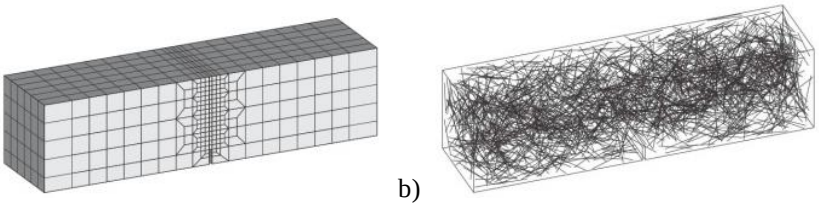

Fig. 2 XFEM modeling of FRC; a) concrete matrix FE mesh, b) randomly dispersed fibers (1D finite elements) [26]

In the last decade more advanced numerical methods are being developed, which include modeling the material on several length scales – thus they are called multiscale methods. To the best of authors' knowledge, these methods have not yet been applied for the FRC modeling, but they are nevertheless mentioned here since the principles they are based on imply that they could successfully be used for this purpose. Namely, there are several types of multiscale methods, but only the most commonly used one will be presented here. In this method the tested specimen is usually considered as a *macro scale model*, and at this level the material is treated as homogeneous. However, its mechanical characteristics are not determined experimentally, but again on a numerical model that represents one small representative part of the macro model – a representative volume element (RVE). This scale is called *meso scale* and on this level all the distinct phases of the material – for example, aggregate, cement paste, voids, etc. - are modeled explicitly and in detail, also taking into account their mutual interactions and connections. Based on the results at the meso scale, the characteristics of the macro scale model are induced and through some homogenization process the required parameters are determined. The described numerical procedure is often referred to as the FE^2 method (Finite Element ^{2}) and it has already been successfully used in solving various problems [28-31]. The principle of deriving the characteristics of a model at one scale based on the analysis of the model at smaller scale can be repeated several times. Thus for instance, the characteristics of a meso scale model can be determined on a micro scale model, and its characteristics could in return be derived from a molecular model (through the use of Molecular Dynamics). In Figure 3a) approximate length boundaries for different scales are given [28], and for the purpose of illustration, in Figure 3b) a schematic representation of the multiscale method application for a concrete beam analysis is shown [29].

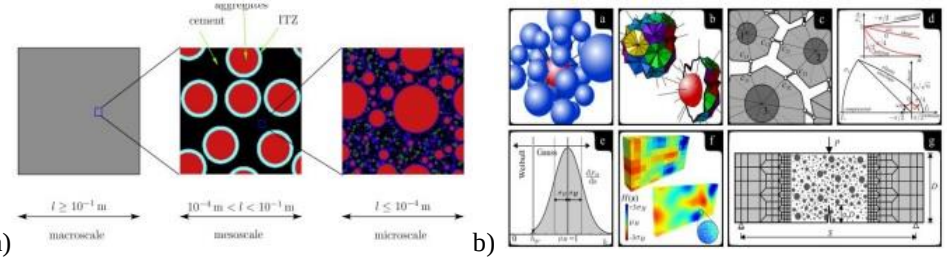

Fig. 3 Multiscale methods, concrete modeling example; a) approximate length scale boundaries [28], b) multiscale modeling of concrete beam [29]

However, although the described methods enable very detailed modeling of material and prediction of its behavior, they are extremely computationally demanding and at this time they have only scientific and research value, but are not applicable in engineering practice.

Here it should be mentioned that there are some relatively recent, nonlocal methods such as peridynamics, where the equations of the Continuum Mechanics are reformulated to include also the nonlocal interaction of parts of the continuum [32,33]. These models are closest to reality since they can model the material behavior on all the length scales simultaneously, but such modeling requires enormous computational resources and is currently used only at some research institutes with massive CPU clusters.

1.3. Problem formulation and a brief paper overview

It can be concluded that the question of effective numerical modeling of FRC remains open and there is no one generally accepted model that would at the same time be sufficiently precise and computationally robust and simple for practical use.

Homogeneous material FRC model is fast, robust, simple and relatively accurate, but the results depend largely on input parameter values, that need to be determined experimentally. On the other hand, more complex, multiscale or non-local models are computationally much too expensive for everyday use.

The combined model with homogeneous matrix and discretely modeled fibers seems like a reasonable compromise between the accuracy and simplicity requirements. In this case, parameters are relatively standard and can be experimentally determined in common tests if necessary. However, in order to produce reliable results, these models require accurate fiber-matrix interaction description, introducing additional parameters and options not readily available in commercial softer packages, so various user-defined subroutines are required, e.g. [24-27]. Therefore, advanced programming skills are needed, which limits the use of these models in everyday engineering practice.

In this paper, a new approach for modeling FRC and numerical prediction of its properties is proposed. The aim is to reduce the amount of required experimental testing in the design of concrete structures, while also bridging the gap between the easy-to-use options readily available in commercial software and the use of a more detailed FRC model with discrete fiber modeling. The proposed approach was developed for Simulia ABAQUS software and it combines XFEM modeling capabilities already included in this software with some other available options for material modeling, in order to produce a fully applicable and sufficiently accurate FRC model without the need for writing complex user defined subroutines.

The proposed numerical modeling procedure was validated against experiment results. Since the main mechanical characteristics of hardened concrete are its compressive and bending tensile strength, these two characteristics were considered in this paper. First, an overview of the experimental testing performed by the authors, in the material testing laboratory of the Faculty of civil engineering and architecture in Niš, Serbia, is given. Next, the proposed numerical model is described in detail, followed by numerical results and their comparison to the experiment and some concluding remarks.

2. EXPERIMENTAL TESTING

2.1. Testing standards and used materials

All tests were done in accordance with the Serbian standards for testing the concrete in its hardened state [34] that were valid on the date of testing. All hardened concrete strengths were tested after 28 days of curing.

2.2. Compression strength

In accordance with [34], a compression strength was tested on cubes of 150x150x150mm dimensions in a standard hydraulic press up to the specimen failure.

2.3. Bending tensile strength

Bending tensile strength was tested on prisms 100x100x400mm, without a notch, in a standard 4-point-bending test. Prisms were simply supported on two steel cylinders symmetrically, with a clear span of 360mm, and loaded by a hydraulic press at thirds of the span, up to the specimen failure.

2.4. Fibers used

In all reinforced specimens, steel hooked fibers were used. The length of fibers was 50mm and their diameter was 1mm. Specific weight of the used steel was 7850 kN/m^3, and its specific tensile strength was 1200N/mm^2. Fiber steel elastic modulus was 210000N/mm^2 and its Poisson's ratio was 0.3.

2.5. Specimen labels, testing procedure and experimental results

In order to evaluate the proposed numerical model, the influence of different quantity of fibers on concrete strengths was tested. Namely, there were 4 series of 3 specimens for the two tested characteristics – 12 cubes and 12 prisms, producing 24 specimens in total. First series of specimens was not reinforced by fibers and it was used for comparison. Specimens of the other 3 series were fiber reinforced, with 0.5%, 1.0% and 1.5% of fiber-to-concrete volumetric share, respectively. Series labels, fiber quantity and experimental results for each series (average of 3 specimens' results) are summarized in Table 1. Specific specimen label consisted of the specimen geometry and series label followed by a specimen serial number, for instance "cube DS0-1", "prism DS5-3", etc. Figure 4 shows some of the tested specimens after the failure.

Fig. 4 Some of the specimens after the test

Table 1 Experimental testing – series labels, fiber quantity and experiment results

Specimen series labels	Fiber quantity (fiber to concr. matrix volumetric share)	Compressive strength (Averaged on 3 cubes) [N/mm^2]	Bending tensile strength (Averaged on 3 prisms) [N/mm^2]
DS0	0.0 %	43.11	6.67
DS4	0.5 %	45.45	7.18
DS5	1.0 %	53.98	10.22
DS6	1.5 %	51.91	10.32

3. The Proposed Numerical Model

All the conducted experimental tests were also modeled numerically, by using Simulia ABAQUS 6.14 software and following the procedure described in the following text.

3.1. Modeling geometry

Two types of numerical models were considered – cubes for compression strength, and prisms for bending tensile strength testing. Cubes dimensions were 150x150x150mm, while prism dimensions were 100x100x400mm. Both models are shown in Figure 5.

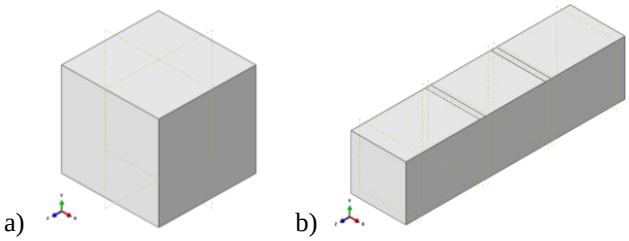

Fig. 5 Geometry of the used numerical models, a) cube for compression strength testing, b) prism for bending tensile strength testing

3.2. Boundary conditions

In the compression strength tests, it was assumed that there was no slip between the steel plate of the press and the contact face of the cube. Thus in numerical modeling, encastre boundary condition (BC) was set on the bottom cube face, and lateral deflections on the top side of the cube were prevented. The load was introduced by incrementally vertically lowering the top cube side for a certain deflection value.

In the bending tensile strength tests, prisms were simply supported, resting on two steel cylinders with a clear span of 360mm between the two contact lines. In numerical models, encastre BC was set along one of these two lines, while on the other the lateral displacements were prevented, and longitudinal were allowed. The load was also introduced through displacements, by vertically lowering the nodes in the region of contact between the prism and the other two cylinders conveying the hydraulic press load.

Boundary conditions for both models are shown in Figure 6.

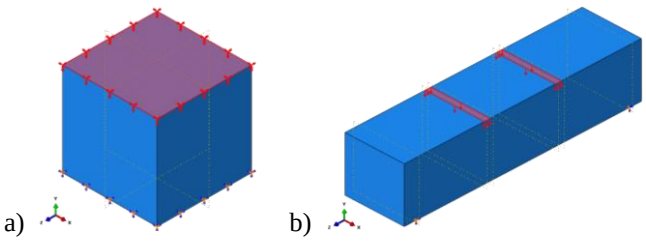

Fig. 6 Boundary conditions for the used numerical models, a) on cubes, b) on prisms

3.3. Finite element mesh for concrete matrix

As the XFEM was utilized, the plain concrete matrix could be meshed independently of the fiber distribution. Thus a regular mesh was adopted for both cube and prism models, using the ABAQUS standard 8-node brick finite element for mechanical analysis of solids. ABAQUS label for this FE type is C3D8R, and it was used with the following options chosen: linear, average strain and first-order accuracy. After the mesh convergence studies, the FE size of 10mm was adopted as both accurate enough and computationally effective. The used FE meshes for cube and prism are shown in Figure 7.

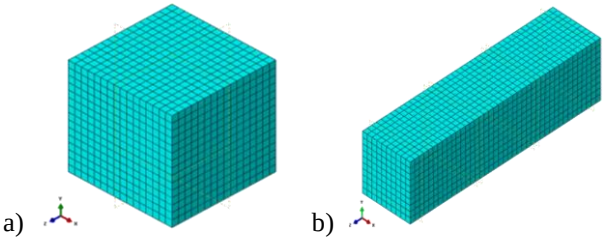

Fig. 7 Finite element meshes for concrete matrix, a) for cubes, b) for prisms

3.4. Material model for concrete

In experimental testing, the concrete mixtures were designed such as to achieve the concrete class of MB40 (The tests were done in accordance with the Serbian standards, the Eurocode equivalent for this concrete class would be approximately C35/45), following the recommendations in the Serbian standard for concrete and reinforced concrete structures design [35]. This fact was used to an advantage in numerical modeling. Namely, all the parameters for the (plain) concrete material model were calculated according to the mentioned standard, for concrete class of MB40. In this way an end-user of the numerical modeling procedure proposed herein only needs to define the targeted concrete class and all the parameters can be calculated without direct experimental testing, while using the wide and thorough tests already done and based on which the Standards were formulated. That been said, the main parameters for the concrete material model are presented in Table 2, along with their values calculated in accordance with [35] for concrete class of MB40.

Table 2 The main parameters for the concrete material model

Material parameter:	Measuring units	Value calculated for MB40 (according to [35])
Elasticity modulus (E_b)	[N/mm^2]	34 000.00
Cube ultimate compressive strength (f_{bk})	[N/mm^2]	43.11
Design compressive strength (f_b)	[N/mm^2]	25.50
Design tensile strength (f_{bz})	[N/mm^2]	3.07
Design bending tensile strength (f_{bzs})	[N/mm^2]	3.82

Stress-strain relation was also adopted in accordance to the mention Standard [35]. The adopted stress-strain diagram is presented in Figure 8.

In tension, tri-linear stress-strain relation was used, with stresses rising linearly with the increase of strain until the tensile strength is reached. Then follows the rapid decrease in stress until the half of the proposed ultimate strain, after which the stresses reduce to zero somewhat more slowly, as can be seen from the diagram.

In compression, the real, pronouncedly nonlinear concrete behavior was approximated by a parabola-straight line as shown on the diagram. The stress is related to strain by:

$$\sigma_b = 0.25 \cdot f_b(4 - \varepsilon_b)\varepsilon_b \tag{1}$$

for $\varepsilon_b \leq \varepsilon_B$, and $\sigma_b = f_b$ for $\varepsilon_B \leq \varepsilon_b \leq \varepsilon_{B2}$, where $\varepsilon_B = 0.2\%$ and $\varepsilon_{B2} = 0.35$. After that point, the stress reduces to zero bi-linearly, as shown.

In Table 3 all the preset stress-strain diagram points are listed for convenience.

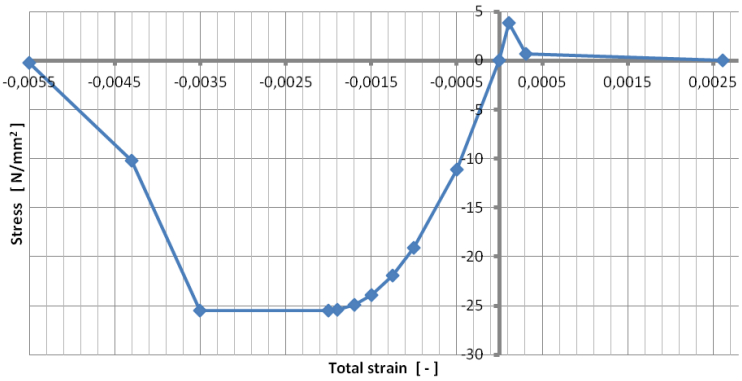

Fig. 8 The adopted stress-strain diagram for plain concrete

Table 3 The preset stress-strain diagram points

Points for the diagram in tension	Stress [N/mm^2]	Total Strain [-]	Plastic strain [-]
Point 1	0	0	-
Point 2	3.82	0.00011	0
Point 3	0.70	0.00031	0.00020
Point 4	0.01	0.00261	0.00250

Points for the diagram in compression	Stress [N/mm^2]	Total Strain [-]	Plastic strain [-]
Point 1	0	0	-
Point 2	11.60	0.00050	0
Point 3	19.13	0.00100	0.00050
Point 4	21.91	0.00125	0.00075
Point 5	23.91	0.00150	0.00100
Point 6	24.93	0.00170	0.00120
Point 7	25.44	0.00190	0.00140
Point 8	25.50	0.00200	0.00150
Point 9	25.50	0.00350	0.00300
Point 10	10.20	0.00430	0.00380
Point 11	0.26	0.00550	0.00500

In ABAQUS, the material model is formed as a combination of one or more elementary material models available in software, each having its own defining parameters. For the numerical modeling proposed in this paper, the concrete material model was obtained by combining two elementary material models – ideally elastic material (IEM) model and concrete damaged plasticity (CDP) model. There are only 2 parameters needed to define IEM model – elasticity modulus and the Poisson's ratio. In this paper, these values were adopted to be 34000N/mm^2 and 0.2, respectively. For CDP model, there are 3 sets of parameters required for material definition. The first group is comprised of the general concrete plasticity parameters and their labels and values adopted for this research are presented in Table 4. The second group of parameters is the set of stress-plastic strain tuples characterizing the points of the stress-strain diagram in compression, and the third one is set of these points for the part of the diagram in tension. Values used in this paper have already been shown in Table 3. No available suboptions for this material model were used.

Table 4 Parameters needed for general concrete plasticity model formulation

Parameter name	Measuring units	Value adopted for this research
Dilatation angle	[-]	31
Eccentricity	[-]	1
fb0/fc0	[-]	1.16
K	[-]	0.6667
Viscosity parameter	[-]	0.001

3.5. Modeling the fibers

The main feature of this paper is the procedure for modeling the fibers of FRC discretely, as a set of 1D FEs randomly distributed in the concrete matrix. As has been previously mentioned, in the current literature there are several papers on this modeling approach [24-27], but in each of them the fiber-matrix interaction is modeled explicitly, through some user defined subroutines. Namely, the XFEM enables that 1D FEs can be introduced regardless of the background concrete matrix mesh (nodes do not have to coincide). However, this method supposes that the embedded FEs are *ideally* bonded with the host region FEs, and it distributes the loads and material responses accordingly. In reality, fiber-matrix bond is achieved through adhesion at the contact interface, and this bond is not ideal. In practice, there are many cases of bond-slipping and fiber pullout, as well as fiber warping or breaking well before the ultimate fiber bearing capacity is reached. These effects largely influence the material response and they have to be accounted for in any numerical model with discrete fibers. This is usually done by including some user defined subroutines as already mentioned. However, these subroutines are often complex and require much knowledge in Continuum mechanics, FEM and ABAQUS syntax, so they cannot be expected to be widely used in everyday practice soon.

In this paper, an attempt was made to capture and model the main phenomena related to fiber-concrete interaction through the use of some options already available in ABAQUS software, avoiding the need for additional scripts. Namely, since the program uses XFEM, the ideal fiber-concrete bond is assumed and bond-slipping and fiber breaking are modeled by defining *separate material models* for each distinct fiber behavior. *Therefore, there were 3 fiber material models (FMM) defined*.

The first FMM (FMM1) simulated the perfect fiber-matrix bond, and the steel fibers were made of was assumed to have linearly elastic-plastic behavior. Thus the FMM1 was obtained by combining linearly elastic solid material model, with elasticity modulus of 210000N/mm^2 and Poisson's ratio of 0.3, and general plastic material model with isotropic hardening. In ABAQUS, the latter material model is also defined through a set of points in a stress-plastic strain diagram. These values were calculated for the yield strength of 1200N/mm^2 and tangent elastic modulus for plastic behavior equal to 1% of the elastic modulus in the elastic region, that is 2100N/mm^2. For plastic strains greater than 0.0163 the strain softening was introduced, so that stresses would decrease to zero at plastic strain of 0.0293. The resulting stress-total strain diagram is shown in Figure 8.

The second FMM (FMM2) was used to simulate the bond-slip and fiber pull-out behavior of the fiber-matrix interaction. The material model was defined in the same way as for the FMM1, only with a lower yield stress limit. After preliminary tests, it was adopted that a fiber would slip at approximately 66% of ideal fiber yielding strength, thus setting the yield strength for FMM2 at 800N/mm2. Also, the tangent elastic modulus was set to zero, and the ultimate plastic strain to 0.01, after which stress gradually decreases to zero at plastic strain of 0.02. The stress-total strain diagram is also presented in Figure 8.

The third FMM (FMM3) was used for fiber breaking simulation. It was the same as FMM1, only that there was no strain hardening after the material yield strength of 1200N/mm^2 was reached. To simulate the breaking behavior, a very steep stress-strain curve was adopted, as can also be seen in Figure 9. Stresses finally reduce to zero at plastic strains of 0.0063.

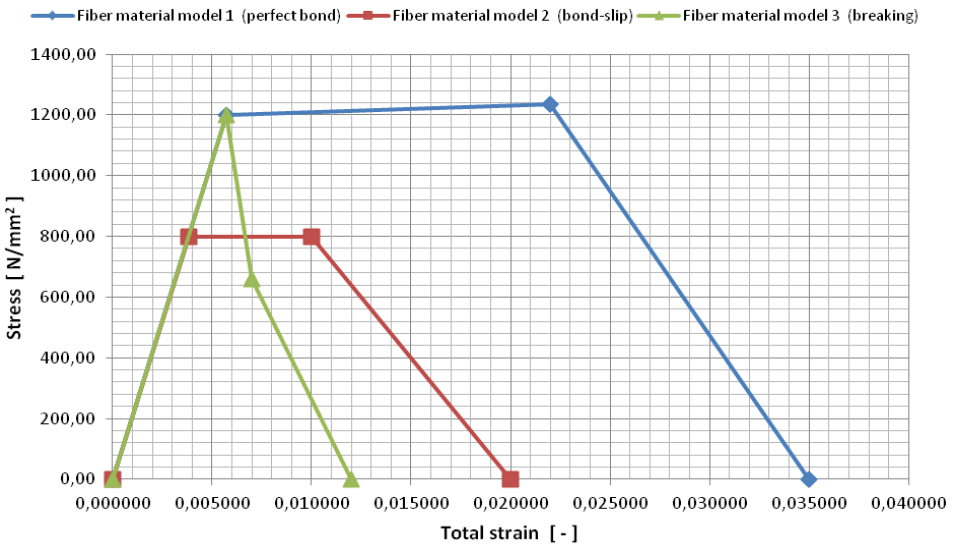

Fig. 9 Stress-strain diagram for the three fiber material models used

When all FMMs are defined, in an analysis each fiber would be randomly assigned one of the FMMs, thus simulating various fiber behaviors. In this way complex fiber-matrix interaction was modeled relatively simply, with no additional subroutines, only by

using the XFEM option already available in the software. Due to a (numerically) perfect bond between the embedded and host FEs, hooks at fibers' ends would have minor or no influence on the solution. Therefore, fibers were model *without the hooks*, as straight cylinders of diameter of 1mm and length of 50mm, approximated with 1D FE of the corresponding characteristics. In ABAQUS, FEs of the type T3D2 were used, which are typical 3D 2-node truss elements for mechanical solid analysis. Number of fibers for each modeled specimen was calculated based on the volume of one fiber and the targeted fiber to matrix volumetric share (described in Section 2).

After the material models, geometry, FE type and total number of fibers were defined, they were randomly dispersed throughout the (already meshed) concrete matrix. The whole modelling procedure proposed in this paper is given as supplementary material in the form of a *python* script, readily executable in the Simulia ABAQUS software. Models obtained in this way for each of the tested FRC specimens are presented in Figure 10.

3.6. Solution procedure and analysis parameters

The load was introduced in 1 step with Maximum number of increments 1000, Initial ("time") increment size 0.01, Minimum increment size 1E-8, and Maximum increment size of 0.01. Direct Newton-Rhapson method was chosen as a solution technique with the geometric nonlinearity taken into account. Adiabatic heating effects were not taken into account, and a general nonlinear static analysis was performed.

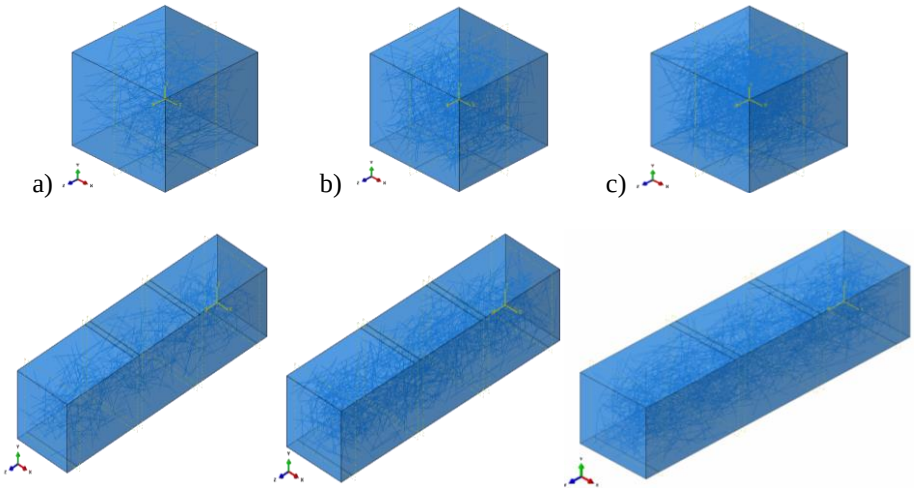

Fig. 10 FRC specimen models, a) 0.5% fibers, b) 1.0% fibers, c) 1.5% fibers

4. RESULTS OF THE NUMERICAL ANALYSIS

The numerical results are displayed in the form of load-displacement diagrams for compressive strength tests and bending tensile strength tests in Figure 11 and Figure 12, respectively. All the results for the compressive strength tests are summarized in Table 5, where the experimentally tested and numerically obtained compressive and bending

tensile strength for all the considered specimens are presented, along with the resulting difference. Similarly, all the results for bending tensile strength tests are summarized in Table 6. (All the results are averaged on at least 3 numerical analyses per specimen.)

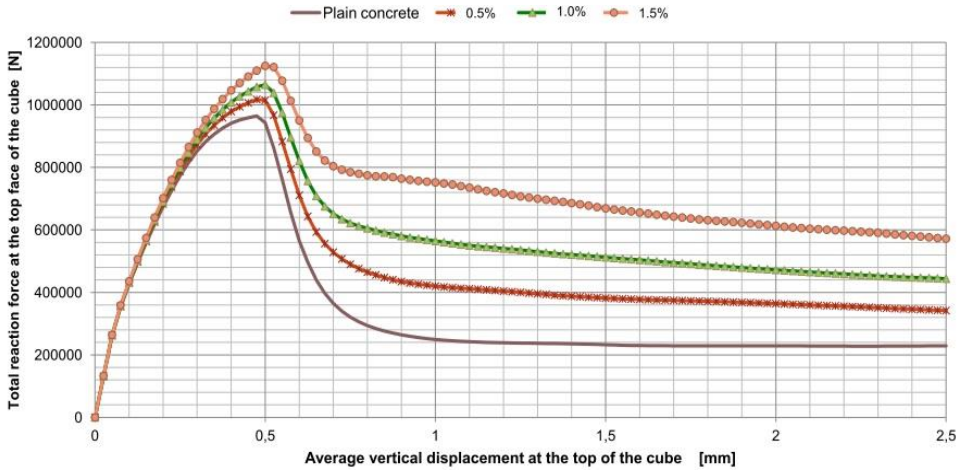

Fig. 11 Load-displacement diagram for compression tests

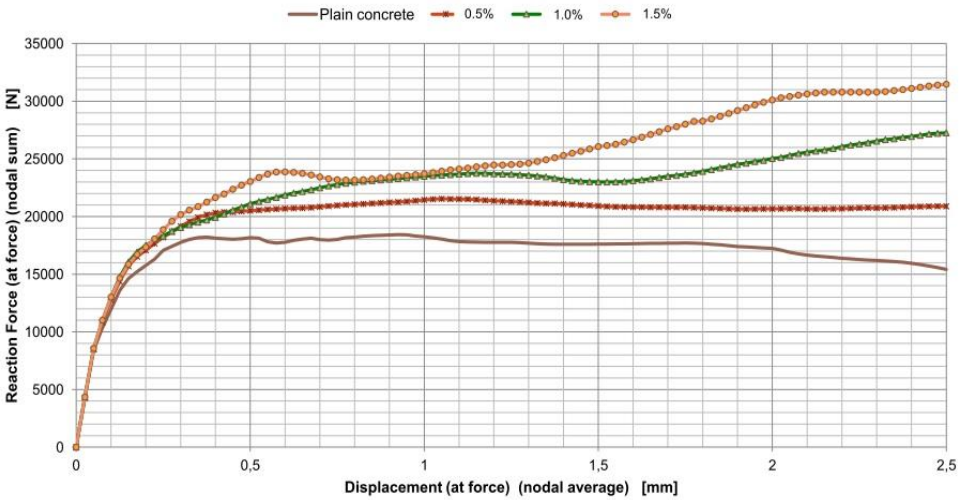

Fig. 12 Load-displacement diagram for bending tensile tests

Table 5 Results summary for compressive strength tests

Specimen series	Fiber to matrix volumetric share	Experimentally determined compressive strength [N/mm^2]	Numerically determined compressive strength [N/mm^2]	Difference
DS0	0.0 %	43.11	42.87	-0.56%
DS4	0.5 %	45.45	45.21	-0.52%
DS5	1.0 %	53.98	47.45	-12.10%
DS6	1.5 %	51.91	50.01	-3.67%

Table 6 Results summary for bending tensile strength tests

Specimen series	Fiber to matrix volumetric share	Experimentally determined bending tensile strength [N/mm^2]	Numerically determined bending tensile strength [N/mm^2]	Difference
DS0	0.0 %	6.67	6.64	-0.50%
DS4	0.5 %	7.18	7.75	+7.96%
DS5	1.0 %	10.22	9.81	-3.98%
DS6	1.5 %	10.32	11.33	+9.77%

4.1. Compressive strength tests comparison

Experimental and numerical results for compressive strength tests are shown in Figure 11 and Table 5. As can be seen from the diagram, the maximum bearing capacity of a specimen can be easily determined in terms of the maximum force the specimen can sustain. Maximum force divided by the area of one face of the cube gives the compressive strength. As it can be seen from Table 5, the results are in a very good agreement with the experiment for all the fiber quantities except for the specimen with 1.0% volumetric share of fibers (VSF). There are several possible explanations to this deviation. The first and the most probable one is that there was a mistake in the experiment, which is indicated by an odd trend – specimen with 1.0% VSF exhibits higher compressive strength (53.98N/mm^2) than the one with 1.5% VSF (51.91N/mm^2). Other possible explanations are also considered in the next Section.

4.2. Bending tensile strength tests comparison

Experimental and numerical results for bending tensile strength tests are shown in Figure 12 and Table 6. It can be concluded from the diagram that the presence of fibers greatly influences the model behavior and increases the specimen bending tensile strength significantly. However, numerical and experimental results differ somewhat more. As can be seen from Table 6, the results are in good agreement for specimens with plain concrete and with 1.0% VSF, while the deviation for specimens with 0.5% VSF and 1.5% VSF is larger. Although higher, deviations still remain within a 10% margin, which was considered acceptable for the numerical model in this stage of development. This deviation could be caused by several factors and these are also considered in the following Section.

4.3. General assessment of the proposed numerical FRC model

From the diagrams in Figure 11 and Figure 12, it can be seen that the general behavior of the proposed numerical model is reasonable and principally acceptable. Some general trends are noticeable:

- Adding more fibers induces higher material strengths.
- Adding more fibers significantly increases the specimen's ductility.
- Specimens' behavior in tension is nonlinear, although a linear stress-strain relation was adopted for plain concrete in tension, which implies a realistic simulation of the influence of the added fibers.
- In tension, for FRC models three distinct stages in material degradation can be observed (and they become more apparent with the increase of VSF) – a mostly linear elastic zone, a gradual material degradation zone, and a complete material degradation zone (horizontal part of the curve) – whereas the plain concrete specimens lack the second one.

Overall, it can be concluded that the proposed model does take into account the influence of fibers on the FRC behavior and it simulates this behavior in a generally acceptable way. However, in its current state of development this model is applicable for global FRC behavior evaluation, but needs improvements in order to describe complex behavior of FRC in detail and, hopefully, to enable numerical prediction of a real FRC behavior with an acceptable accuracy. Some of these improvements are discussed in the next Section.

5. CONCLUDING REMARKS

5.1. Result analysis and evaluation of the proposed model

In this paper a FRC model with discrete fiber modeling by using the Simulia ABAQUS software is presented. An alternative way to define the fiber-concrete matrix interaction is proposed and the obtained numerical results are validated against the results of the conducted experimental tests, for specimens with various volumetric shares of fibers. Numerical results are mostly in good agreement with the experiment, but there are relatively large deviations for some tested specimens. There are several possible reasons for this deviation:

Erroneous experiment – some unexpected trends are observed in both compression and bending tensile strength results. For instance, it appears as the specimen with 1.0% VSF has higher compression strength than the one with 1.5% VSF. Furthermore, the increase in bending tensile strength between the specimen with 1.0% VSF (10.22N/mm^2) and the one with 1.5% VSF (10.32N/mm^2) is very small (approx. 1%) compared to the increase between other specimens (average increase is approx. 30%), and the strength is much lower than expected. This could explain the considerable numerical error.

Random fiber distribution – since the fibers are modeled explicitly and are distributed *randomly* throughout the concrete matrix, this model is bound to produce somewhat different results with each performed analysis. Thus it is necessary to repeat the analysis many times in order to obtain a valid statistical average/mean result. Therefore, additional analyses were performed and a promising trend was observed. For example, the deviation in bending tensile strength for the specimen with 0.5% VSF was initially 12.56%, but after taking the average of 8 analyses it reduced to the presented value of 7.98%. This implies that the model could converge to a more accurate solution with an increased number of analyses. However, one of the main disadvantages of this modeling approach exhibits itself here – since the fibers are modeled discretely, the analysis is much more computationally expansive, and due to relatively limited computational resources, repeating the analysis sufficient number of times to produce a statistically significant population would require a very large amount of time. For illustration purposes, in Table 7 the evaluation time for models with different VSF is summarized. The analyses were

done on a PC with Intel i5-7400 CPU 4x3.0GHz and 8.0 GB RAM. As it can be seen, the total evaluation time increases exponentially with the increase of volumetric share of fibers. Nevertheless, although with the current result the deviation in the results remains considerable, it is possible that it would diminish with larger number of repeated analyses, and this could be easily achieved with higher computational power.

Table 7 Average evaluation time in seconds for a single model of various type and VSF

Specimen	DS0 (0%)	DS4 (0.5%)	DS5 (1.0%)	DS6 (1.5%)
cube	182	2552	6192	10088
prism	562	2266	6480	10804

Insufficiently accurate fiber bond-slip behavior modeling – in this paper, fiber-matrix interaction was modeled through the use of different fiber material models (FMMs), and three distinct behaviors were considered – a perfect bond with yielding of fibers, a fiber-pullout with a bond-slip defect, and a fiber breaking. However, the bond-slip and fiber-pullout can occur at different stress levels, depending on the realized fiber-concrete adhesion. Various factors such as fiber geometry, concrete material structure in fiber area and cement hydration in vicinity of fiber influence this adhesion, making it very hard to predict the exact bond-slip stress (BSS) level. In this paper, after some preliminary analyses, BSS was adopted to be equal to two thirds of the fiber steel yield strength. Generalization of this type could have caused the mentioned numerical solution deviations. However, this is not very likely, since the results are in good agreement with the experimental ones for the rest of the considered specimen types.

Some other phenomena unaccounted for in this model – the proposed model considers some of the specific fiber-matrix and concrete behavior phenomena. However, many idealizations were also made, for instance: concrete matrix is modeled as a homogeneous material, fibers are geometrically perfect and evenly distributed (though randomly oriented) inside the matrix, and so on. Moreover, some phenomena such as concrete-wall interlocking effect and some others, perhaps yet undiscovered effects were neglected. These phenomena could also have led to the considered results deviation.

5.2. Possible improvements of the proposed model

In its current state of development, the proposed model produces results in reasonable agreement with the experiment. However, it can be greatly improved by introducing accurate fiber geometry (hooked end fibers) and a more precise fiber-matrix interaction, especially regarding the bond-slip behavior, and randomizing the bond-slip stress level within a certain range to simulate different possible conditions of fiber-matrix interface.

5.3. General conclusions and suggested directions for further research

The numerical FRC model proposed in this paper is robust, relatively accurate and simple to use, presenting a successful alternative to the commonly used models, and it can be improved to make it an even more accurate and comprehensive FRC model.

However, although promising, this model has certain drawbacks inherent to all the models of the discrete fiber modeling approach. It requires considerable computational resources to evaluate the model, and due to the random fiber distribution it requires many repeated analyses to derive statistically conclusive results. Moreover, it is not yet reliable

enough to make accurate predictions that could provide a firm basis for structural design. This, combined with the high computational requirements, renders this model not yet applicable in engineering practice, thus partially neutralizing the advantage gained by simplifying a discrete fibers model and bringing it closer to a wider circle of end-users.

After all that was said, authors would still suggest that further research be mainly oriented towards improving and further developing the homogenous material FRC model, while models with discrete fibers such as the one proposed in this paper could be used to numerically estimate the parameters required for the homogeneous material model definition, thus reducing or even completely avoiding the need for experimental tests, which would make the design process cheaper and more efficient. In this way the advantages of both modeling approaches would be combined and they would complement each other, and the model proposed here could help in achieving this goal.

Acknowledgement. *Parts of this research were supported by the Ministry of Sciences and Technology of Republic of Serbia, through the Mathematical Institute of SASA, Belgrade.*

REFERENCES

1. Ranković, S., Folić, R., & Mijalković, M. (2010). "Effects of RC beams reinforcement using near surface mounted reinforced FRP composites". Facta universitatis - series: Architecture and Civil Engineering, 8(2), 177-185.
2. Lepenies, I. G., Richter, M., & Zastrau, B. W. (2008, December). "A Multi-Scale Analysis of Textile Reinforced Concrete Structures". In PAMM: Proceedings in Applied Mathematics and Mechanics (Vol. 8, No. 1, pp. 10553-10554). Berlin: WILEY-VCH Verlag.
3. Krishna, R., Kumar, R. P., & Srinivas, B. (2011). "Effect of size and shape of specimen on compressive strength of glass fiber reinforced concrete (GFRC)". Facta Universitatis-Series: Architecture and Civil Engineering, 9(1), 1-9.
4. A.M.Brandt, "Fiber reinforced cement-based (FRC) composites after over 40 years of development in building and civil engineering", Composite Structures, vol. 86, pp. 3-9, 2008
5. D.Snoeck, N. De Belie, "From straw in bricks to modern use of microfibers in cementitious composeites for improved autogenous healing – A review", Construction and Building Materials, vol. 95, pp. 774-787, 2015
6. R.F.Zollo, "Fiber-reinforced Concrete: an Overview after 30 years of Development", Cement and Concrete Composites, vol. 19, pp. 107-122, 1997
7. T. Blaszczynski, M. Przybylaska-Falek, "Steel fiber reinforced concrete as a structural material", Pricedia Engineering, vol. 122, pp. 282-289, 2015
8. B. Mobasher, Y. Yao, Ch. Soronakom, "Analytical solutions for flexural design of hybrid steel fiber reinforced concrete beams", Engineering Structures, vol. 100, pp. 164-177, 2015
9. H. Behbahani, B. Nematollahi, "Steel Fiber Reinforced Concrete: A Review", conference paper, December 2011, downloaded from Research Gate on August 24th 2018. https://www.researchgate.net/publication/266174465_Steel_Fiber_Reinforced_Concrete_A_Review
10. Jekic, Zakic, Savic (2008) MODELING OF PROPERTIES OF FIBER REINFORCED CEMENT COMPOSITES
11. Predrag Blagojević, PhD thesis (2011) Faculty of Civil Engineering and Arcitecture, University of Niš, Serbia
12. Eik, M., Puttonen, J., & Herrmann, H. (2015). "An orthotropic material model for steel fibre reinforced concrete based on the orientation distribution of fibres". Composite Structures, 121, 324-336.
13. Mobasher, B., Yao, Y., & Soranakom, C. (2015). "Analytical solutions for flexural design of hybrid steel fiber reinforced concrete beams". Engineering Structures, 100, 164-177.
14. Salehian, H., & Barros, J. A. (2017). "Prediction of the load carrying capacity of elevated steel fibre reinforced concrete slabs". Composite Structures, 170, 169-191.
15. D.M.Ozcan et al., "Experimental and finite element analysis of the steel fiber-reinforced concrete (SFRC) beams ultimate behavior", Construction and Building Materials, vol. 23, pp. 1064-1077, 2009
16. R. Ceroni et al., "A general 3D approach for the analysis of multi-axial fracture behavior of reinforced concrete elements", Engineering and Fracture Mechanics, vol. 78, pp. 1784-1793, 2011

17. A.Brighanti et al., "Cracking behavior of fiber reinforced cementitious composites: A comparison between continuous and a discrete computational approach", Engineering and Fracture Mechanics, vol. 103, pp. 103-114, 2013
18. D. Nicolaides, G. Markou, "Modelling the flexural behavior of fiber reinforced concrete beams with FEM", Engineering Structures, vol. 99, pp. 653-665, 2015
19. Luccioni, B., Ruano, G., Isla, F., Zerbino, R., & Giaccio, G. (2012). "A simple approach to model SFRC". Construction and building materials, 37, 111-124..
20. Mihai, I. C., Jefferson, A. D., & Lyons, P. (2016). "A plastic-damage constitutive model for the finite element analysis of fibre reinforced concrete". Engineering Fracture Mechanics, 159, 35-62.
21. Singh, M., Sheikh, A. H., Ali, M. M., Visintin, P., & Griffith, M. C. (2017). "Experimental and numerical study of the flexural behaviour of ultra-high performance fibre reinforced concrete beams". Construction and Building Materials, 138, 12-25.
22. Mark, P., & Bender, M. (2010). "Computational modelling of failure mechanisms in reinforced concrete structures". Facta universitatis-series: Architecture and Civil Engineering, 8(1), 1-12.
23. Jefferson, A. D., Mihai, I. C., Tenchev, R., Alnaas, W. F., Cole, G., & Lyons, P. (2016). "A plastic-damage-contact constitutive model for concrete with smoothed evolution functions". Computers & Structures, 169, 40-56
24. V. M.C.F. Cunha, J. A.O. Barros, J. M. Sena-Cruz, "A finite element model with discrete embedded elements for fibre reinforced composites", Computers and Structures, vol. 94-95, pp. 22-23, 2012
25. J. Kang, K. Kim, Y. Mook Lim, J. E. Bolander, "Modeling of fibre-reinforced cement composites: Discrete representation of fiber pullout", International Journal of Solids and Structures, vol. 51, pp. 1970-1979, 2014
26. V. M.C.F. Cunha, "Steel Fiber reinforced Self-Compacting Concrete (from Micro-Mechanics to Composite Behavior)", PhD thesis, University of Minho, Portugal (2010) ISBN: 978-972-8692-44-5
27. Radtke, F. K. F., Simone, A., & Sluys, L. J. (2010). "A computational model for failure analysis of fibre reinforced concrete with discrete treatment of fibres". Engineering fracture mechanics, 77(4), 597-620.
28. V.P. Nguyen, M. Stroeven, L.J. Sluys, "Multiscale failure modeling of concrete: Micromechanical modeling discontinuous homogenization and parallel computations", Computational Methods and Aplications in Mechanical Engineering, vol. 201-204, pp. 139-156, 2012
29. J. Elias, M. Vorechovsky, J. Skoček, Z. P. Bažant, "Stochastic discrete meso-scale simulations of concrete fracture: Comparison to experimental data", Engineering Fracture Mechanics, vol. 135, pp. 1-16, 2015
30. V. Palmieri, L. De Lorenzis, "Multiscale modeling of concrete and of the FRP-concrete interface", Engineering Fracture Mechanics, vol. 131, pp. 150-175, 2014
31. H. M. Jennings, J. W. Bullard, "From electrons to infrastructure: Engineering concrete from bottom up", Cement and Concrete Research, vol. 41, pp. 727-735, 2011
32. A. Yaghoobi, M. G. Chorzepa, "Fracture analysis of fiber reinforced concrete structures in the micropolar peridynamic analysis framework", Engineering Fracture Mechanics, vol. 169, pp. 238-250, 2017
33. W. Gerstle, N. Sau, S. Silling, "Peridynamic modeling of concrete structures", Nuclear Engineering and Design, vol. 237, pp. 1250-1258, 2007
34. SRPS EN 12390-1:2016, SRPS EN 12390-2:2016, SRPS EN 12390-3:2016, SRPS EN 12390-5:2016
35. Pravilnik o tehničkim normativima za beton i armirani beton PBAB87, "Službeni list SFRJ", br 15/90

PREDLOG NOVOG NUMERIČKOG MODELA ZA ODREĐIVANJE ČVRSTOĆE BETONA OJAČANOG VLAKNIMA

U ovom radu je prikazan alternativan numerički model za određivanje čvrstoće betona ojačanog vlaknima na pritisak i na zatezanje savijanjem. Vlakna su modelirana diskretno, koristeći Prošireni Metod Konačnih Elemenata (Extended Finite Element Method – XFEM). Predložen je i novi način modeliranja interakcije između vlakana i betonske matrice, bez potrebe za definisanjem dodatnih podrutina.Predloženi numerički model proveren je prema ekxperimentalnim ispitivanjima i rezultati se slažu u zadovoljavajućim granicama. Model je razvijen za rad u Simulia Abakus softveru (Simulia ABAQUS), ali je prikazana procedura opšte primenljiva. Na kraju su izložena i moguća unapređenja modela i predlozi njegove primene.

Ključne reči: *beton ojačan vlaknima, mikroarmirani beton, XFEM, model sa diskretnim vlaknima, interakcija vlakna i betona, numeričko određivanje čvrstoća*